Permanent deformation estimates of dynamic equipment foundations: Application to a gas turbine in granular soils

Rubén Galindo , Manuel Illueca , Rafael Jimenez

A B S T R A C T

Permanent displacements of a gas turbine founded on a fine, poorly graded, and medium density sand are studied. The amplitudes and modes of vibration are computed using Barkan´s formulation, and the "High-Cycle Accumulation" (HCA) model is employed to account for accumulated deformations due to the high number of cycles. The methodology is simple: it can be easily incorporated into standard mathematical software, and HCA model parameters can be estimated based on granulometry and index properties. Special attention is devoted to 'transient' situations at equipment´s start-up, during which a range of frequencies – including frequencies that could be similar to the natural frequencies of the ground – is traversed. Results show that such transient situations could be more restrictive than stationary situations corresponding to normal operation. Therefore, checking the stationary situation only might not be enough, and studying the influence of transient situations on computed permanent displacements is needed to produce a proper foundation design.

Keywords:
Machinery
Permanent deformations
High number cycles
Cyclic loading

1. Introduction

Cyclic loads acting on a foundation element are transmitted to the ground, producing strains that may induce settlements. Such settlements need to be controlled for an adequate functionality of foundations and of their overlaying equipments. Previous research on the cyclic behavior of sands has mainly considered seismic loading: i.e., short and intense cyclic-loads that may produce liquefaction, permanent deformations, or both. But machine foundations are different, since vibration amplitudes are usually small and do not produce substantial short-term deformations. For instance, in foundations on non-saturated soils, appreciable permanent deformations could occur as a result of dynamic amplifications due to matching of the natural vibration frequencies of the soil and the equipment; or, as indicated by Okur and Ansal [1], to 'stiffness degradation' –the rapid growth of deformation that occurs when a certain number of cycles of a given amplitude act on the soil [2]– produced by the high number of load cycles.

To avoid resonance problems, it is common that manufacturers suggest that the mass of the foundation is 2–3 times the mass of the vibrating machine. However, such approach is often heuristic, as a larger foundation mass does not necessarily imply smaller vibrations [3]. Building on previous research, Anyaegbunam [3] has recently proposed methods to select foundation mass to limit vibrations. Such solutions, however, assume the damped vibration of a single degree of freedom (SDOF) analog, hence neglecting cyclic soil behavior.

In this work, permanent deformations (displacements) of a gas turbine founded on granular soils are studied, considering both normal 'steady-state' operation and 'transient-states', such as those occurring during start-up and switch-off. (A recent similar analysis is presented by Francois et al. [4], who considered accumulated foundation settlements in granular soils due to traffic loading.) The explicit "High-Cycle Accumulation" (HCA) model [5,6] is used to estimate deformations in this work. Since the model is simple to program and use, with parameters that can be estimated using common geotechnical information – mainly, granulometry (grain size, uniformity), and index properties (minimum void ratio) [7] – it can be employed, even at initial stages of a project, for simple settlement estimations of foundations for vibratory equipment, such as those commonly employed for turbines in energy projects.

2. Project description

2.1. Geotechnical characterization and geometry of the gas turbine foundation

We study the foundation of a gas turbine – and its auxiliary equipments – in a combined-cycle energy plant. The turbine

foundation is constructed using a concrete block with weight $W=24{,}699$ kN. The block is symmetric along its longitudinal axis, with $L=43$ m length, and with variable width, B, with $B=8$ m below the control units and the generator, and with B reaching $B=12.8$ m under the turbine. (The average width is $B_{av}=9.07$ m). See Fig. 1 for a schematic representation of the foundation layout, and Fig. 2 for a cross section.

Available geotechnical data, including SPT measurements, show that the turbine is founded on a fine, poorly graded, and medium density sand, which is homogeneous with depth. It has a uniformity coefficient of $C_u=4.2$, a coefficient of curvature of $C_c=0.92$, and an average grain size $d_{50}=0.32$ mm. Its minimum void ratio, corresponding to 'maximum density' conditions, is $e_{min}=0.40$, and the maximum is $e_{max}=0.70$, with an in-situ void ratio of 0.50, critical friction angle of 30° and a bulk density of 18 kN/m^3. The water table is deep enough so as not to affect the foundation performance.

A cross-hole test was conducted to characterize the ground´s dynamic elastic parameters. Results are presented in Fig. 3, which suggests an approximately linear increase with depth. Given such data, representative average values for the dynamic 'stress bulb' below the foundation, corresponding to approximately 1.5 times the foundation width ($1.5B=13.5$ m), are selected. Thus, the following parameters, that correspond to the arithmetic average of available field data, will be adopted as representative for dynamic design: Poisson ratio 0.3, elastic Young´s modulus 729 MPa, and Shear modulus 279 MPa. Due to the small strain amplitudes generated in the soil by the gas turbine, an amplitude dependence of these dynamic parameters is not considered in the present study. In addition, on the side of safety, the increase of the stress in the subsoil due to the weight of the vibratory equipment, and of its foundation, is not considered to obtain such representative elastic values.

2.2. Vibration of the gas turbine

The eccentricity of a rotating mass with respect to its rotation axis produces dynamic loads that depend on the mass, and on the angular velocity, of the rotating device. In our case, the dynamic loads are due to the turbine and the generator; since they have the same rotation velocity, they can be considered as a unique dynamic load, and they will jointly referred to as the 'turbine' load.

The manufacturer provides the 'equivalent' magnitude of the (centrifugal) force produced by the turbine in the stationary regime. It can be computed as:

$$P_0 = \frac{\pi W_L N_m}{980} \tag{1}$$

where P_0 is the magnitude of the equivalent centrifugal force (kN), W_L is the weight of the rotating mass (kN) and N_m is the rotation frequency (Hz). (See Table 1 for values corresponding to the equipments considered herein).

However, gas turbines can also produce transient situations with variable rotation frequency. As an example, Fig. 4 shows the evolution with time of the turbine´s vibration frequencies during 'start-up': first, there is a fast frequency increase, reaching approximately 600 rpm after 100 s; then, there is a 360 s period with constant vibratory frequency that corresponds to the 'purging' or 'cleaning' of the turbine; and, finally, the frequency increases almost linearly until it reaches, after approximately 28 min (1680 s), its steady-state (normal operation) value of 3600 rpm (60 Hz). Below, it is shown that these transient situations can have a significant contribution to permanent deformations.

3. Dynamic analysis of the foundation

To study the dynamic behavior of the ground, we first need to compute its response – amplitudes and modes of vibration – as a result of the (harmonic) dynamic loads introduced by the vibratory equipment. Traditionally, such analyses have been conducted using Barkan´s formulation [8], which assumes a vibratory mass on elastic ground, *as neglecting damping is simpler and on the side of safety*.

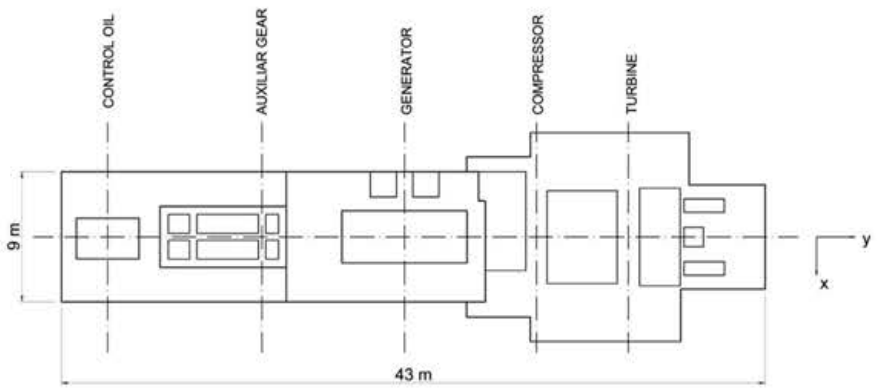

Fig. 1. Simplified geometry of the gas turbine foundation (plan view).

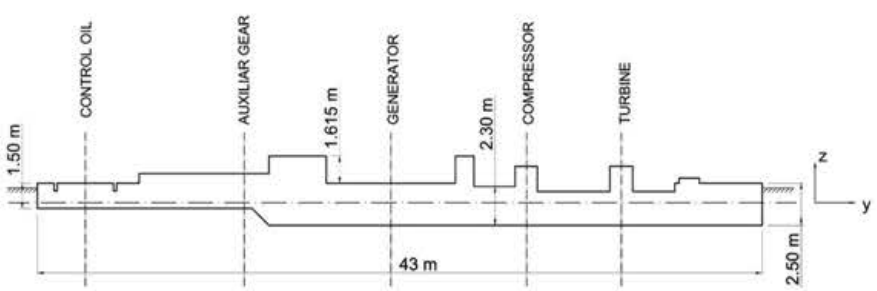

Fig. 2. Cross section of the turbine foundation.

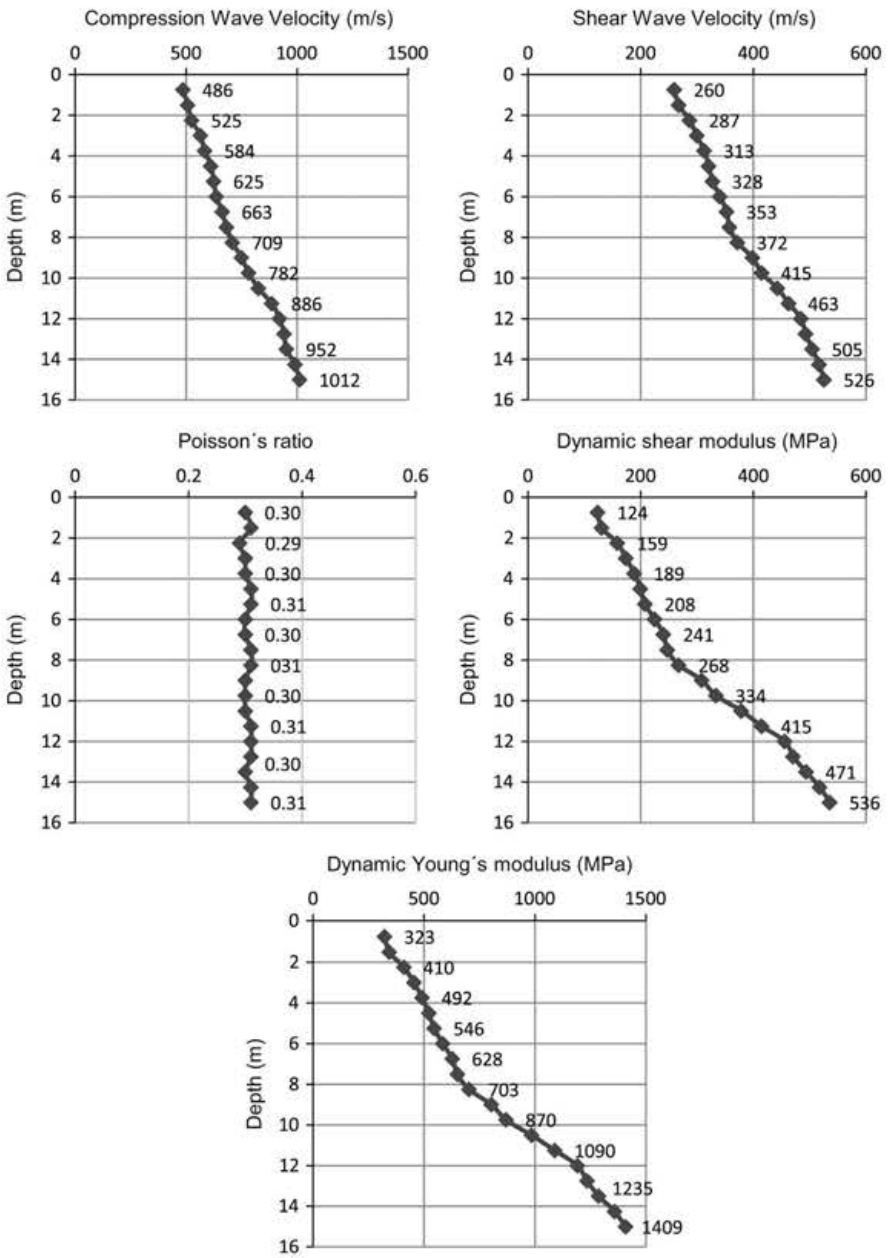

Fig. 3. Dynamic properties of the ground.

Table 1
Physical characteristics of the generator and turbine.

	W_L	N_m		P_0
Generator	520 kN	3600 rpm	60 Hz	100.02 kN
Turbine	481 kN	3600 rpm	60 Hz	92.52 kN

In general, a foundation can be modeled as a 'block' with 6 vibration modes: three rotations and three displacements. In this case, however, since the turbine´s axis of rotation is aligned with the foundation´s symmetry axis, the number of vibration modes is reduced to 3: two displacements along the x and z axes, and one rotation around the y axis (see Figs. 1and 2 for a definition of axis directions). Fig. 5 shows that, when a moment M_y acts, the foundation motion (shown in Fig. 5a, where M_r and P_r are the resisting moment and force) is equal to the sum of a horizontal and a rocking motion (Figs. 5b and c, respectively). Furthermore, the vertical translation mode is decoupled from the others; whereas horizontal displacement and rotation are coupled [9].

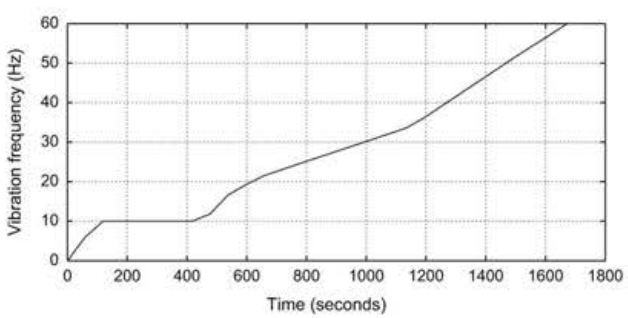

Fig. 4. Evolution of frequencies with time during start-up of the turbine.

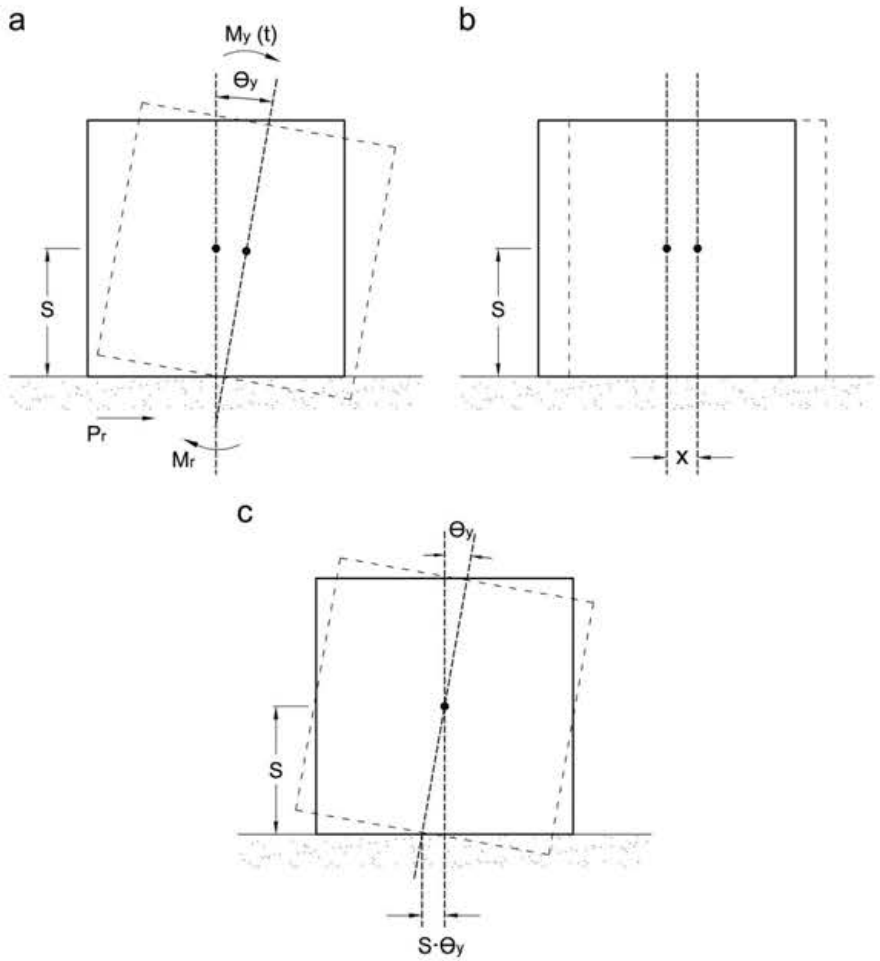

Fig. 5. Coupled rocking and sliding vibration.

The dynamic equations governing the foundation behavior are: Equation of vertical motion:

$$m\ddot{z}+K_z z=P_z(t) \tag{2}$$

Equation of horizontal motion:

$$m\ddot{x}+K_x(x-S\theta_y)=P_x(t) \tag{3}$$

Equation of rotation about the y axis:

$$I_y\ddot{\theta}_y-K_xSx+(K_\theta-WS+K_xS^2)\theta_y=M_y(t) \tag{4}$$

where m and W represent the mass and weight of the foundation; K_z, K_x, and K_θ represent the ground 'stiffness' for each vibration mode; and P_z, P_x and M_y represent magnitudes of excitations (forces and moments) for each vibration mode. S is the distance from the foundation base to the center of gravity of the vibratory equipment and I_y is its moment of inertia about the y axis. (Obviously, the moment M_y produced by the rotating load, P_0, is computed multiplying P_0 times the distance between the center of gravity of the rotating machine and its rotation axis).

The stiffness constants for each vibration mode can be computed from the dynamic elastic parameters (G and ν), the dimensions of the foundation (B and L), and three additional parameters (α_z, α_x and α_θ), available from [8], which depend on the ratio B/L. They are:

$$K_z=\frac{G}{1-\nu}\alpha_z\sqrt{BL} \tag{5}$$

$$K_x=2(1+\nu)G\alpha_x\sqrt{BL} \tag{6}$$

$$K_\theta=\frac{G}{1-\nu}\alpha_\theta BL^2 \tag{7}$$

Applying the above equations for this case study produces the following:

$$\ddot{z}=-5997.1z+1.23\times10^{-3}f\ \sin(2\pi ft) \tag{8}$$

$$\ddot{x}=-5457.4(x-1.78\theta_y)+1.23\times10^{-3}f\ \cos(2\pi ft) \tag{9}$$

$$\ddot{\theta}_y=602.3x-14439.2\theta_y+3.28\times10^{-4}f\ \cos(2\pi ft) \tag{10}$$

where $f=60$ Hz for the stationary regime. For the start-up situation, the variation of the frequency f (Hz) with time t (s) would be (see Fig. 4):

$$f=\begin{cases}0.1t;\ t\in[0,100]\\ 10;\ t\in(100,460]\\ 0.1032t-37.46;\ t\in(460,502]\\ 0.0648t-18.20;\ t\in(502,538]\\ 0.0434t-6.68;\ t\in(538,634]\\ 0.0278t+3.22;\ t\in(634,664]\\ 0.0253t+4.90;\ t\in(664,1126]\\ 0.0347t-5.76;\ t\in(1126,1162]\\ 0.0504t-23.99;\ t\in(1162,1534]\\ 0.0417t-10.58;\ t\in(1534,1558]\\ 0.0497t-23.11;\ t\in(1558,1672]\\ 60;\ t\in(1672,1732]\end{cases} \tag{11}$$

Solving these differential equations provides the evolution with time of the foundation's displacements (z and x, in meters) and rotation (θ_y, in radians). (In this case, second and third order Runge–Kutta solvers available in MATLAB are employed.) Also, once the stiffness constants are available, the natural frequencies for each vibration mode can be computed. In our gas turbine foundation, they are: 12.3 Hz for the vertical vibration, 11.76 Hz for the horizontal vibration, and 16.82 Hz for the rocking vibration.

4. Models for prediction of strain accumulation

Barkan's equations solve the (elastic) dynamic problem: Although they consider dynamic amplifications, they neglect damping and do not consider accumulated permanent deformations due to cyclic loads. Neglecting damping is conservative, but neglecting accumulated deformations is not. To account for accumulated deformations, displacements and rotations computed from Barkan's equations need to be transformed into stresses and strains and, through an adequate soil behavior model, into permanent strain estimates from which permanent displacements can be computed.

Vertical and horizontal stresses (σ_z and σ_x) and strains (ε_z and ε_x) can be computed from the vertical and horizontal displacements (z and x) and the rotation (θ_y) as:

$$\sigma_x = \frac{K_x x}{BL};\ \sigma_z = \sigma_{zv} + \sigma_{zh} = \frac{K_z z}{BL} + \frac{K_\theta \theta_y B}{4 I_y} \tag{12}$$

$$\varepsilon_x = \frac{1}{E}(1+\nu)[(1-\nu)\sigma_x - \nu\sigma_z]: \quad \varepsilon_z = \frac{1}{E}(1+\nu)[-\nu\sigma_x + (1-\nu)\sigma_z] \tag{13}$$

The most common types of models for cyclic soil behavior are 'implicit models' and 'explicit models'. Implicit models consider, by an incremental law in successive time steps, the complete evolution of stresses and strains. Examples include models with nested yield surfaces [10–12]; endochronic models [13–15]; boundary surface models [16–18]; hypoplastic models [19–21]; and models based on Generalized Plasticity Theory [22]. Anastasopoulus et al. [23] recently presented a simple constitutive model with kinematic hardening for soil behavior, and they used it to estimate the cyclic response of shallow foundations under strong (seismic) shaking. Although these models have been successfully applied to processes such as stiffness degradation and densification of soils, they require a large computational effort even for simple problems. And the accumulation of numerical errors could be significant when the number of cycles is high (say, $> 10^3$), as it happens during the design life of vibratory equipment.

Explicit models are an alternative. They explicitly evaluate cyclic strain accumulation after a large number of small amplitude cycles (up to several million), with two main formulations: power laws of the number of cycles [24–28], and logarithms of the number of cycles [5,6,29]. Explicit models usually consider a dependence of the rate of strain accumulation on state (i.e. stress, density, ...) and on cyclic loading history. The model parameters depend mainly on soil type and can be estimated through laboratory or field testing. But, being empirical, the performance of an explicit model will depend on the similarity, between 'calibration' and 'field' conditions, of soil state (e.g., initial density and stress) and load characteristics (amplitude, direction, etc.). For instance, since Suiker [30] and Wichtmann [31] showed that strain continues to accumulate even after millions of cycles, the experimental program conducted to calibrate the model should cover that range of cycle numbers. In addition, the model should incorporate the influence of the decrease of the rate of strain accumulation with decreasing void ratio.

We use the HCA model [5,6] to estimate permanent displacements of the turbine foundation. The HCA model is an empirical explicit model that builds on the work of Sawicki and Swidzinski [29], adding new parameters and improving the formulation to provide the direction of accumulated strains. It can represent, with a high reliability, the dynamic ground behavior under large number of cycles ($> 10^3$), with small or moderate total strain amplitudes ($< 10^{-3}$). It is based on many cyclic triaxial tests conducted with granular soils that allowed the authors to assess the influence of many factors – e.g, amplitude and frequency of strain cycles, average stress, void ratio, load history, number of cycles, polarization of the cyclic load, etc. – on permanent strains, and to derive simple expressions for calibration using only granulometric and state variables.

The HCA model considers that stresses and strains resulting from cyclic loading can be decomposed into an oscillatory part, described by the amplitude of strain, and by a cumulative strain part. The general expression is [5,6]:

$$\dot{\boldsymbol{\sigma}} = \boldsymbol{E} : (\dot{\boldsymbol{\varepsilon}} - \dot{\boldsymbol{\varepsilon}}^{\boldsymbol{acc}} - \dot{\boldsymbol{\varepsilon}}^{\boldsymbol{pl}}) \tag{14}$$

Where $\dot{\boldsymbol{\sigma}}$ represents the rate of effective stress, $\dot{\boldsymbol{\varepsilon}}$ is the rate of strain, $\dot{\boldsymbol{\varepsilon}}^{\boldsymbol{acc}}$ is the rate of accumulative (permanent) strain, $\dot{\boldsymbol{\varepsilon}}^{\boldsymbol{pl}}$ is the plastic strain rate, and $\boldsymbol{E}$ is the matrix of elastic deformation moduli. (Note that, within the HCA framework, 'variations' or 'rates' represent 'derivatives' with respect to the number of cycles).

The HCA model computes the accumulated (permanent) strain, $\dot{\boldsymbol{\varepsilon}}^{\boldsymbol{acc}}$, as:

$$\dot{\boldsymbol{\varepsilon}}^{\boldsymbol{acc}} = \dot{\varepsilon}^{acc}\boldsymbol{m} \tag{15}$$

where $\boldsymbol{m}$ is a unit tensor that indicates the direction of the accumulated strain. Experimental evidence suggests that the Modified Cam Clay flow rule is an adequate approximation of $\boldsymbol{m}$:

$$\boldsymbol{m} = \frac{-\frac{1}{3}\left(p^{av} - \frac{(q^{av})^2}{M^2 p^{av}}\right)\boldsymbol{I} + \frac{3}{M^2}\boldsymbol{\sigma}^*}{\left\| -\frac{1}{3}\left(p^{av} - \frac{(q^{av})^2}{M^2 p^{av}}\right)\boldsymbol{I} + \frac{3}{M^2}\boldsymbol{\sigma}^* \right\|} \tag{16}$$

with p^{av} and q^{av} being Roscoe invariants calculated from average stress σ^{av}, $\boldsymbol{I}$ the unit tensor, σ^* the deviator part of Cauchy stress tensor and M the Cam Clay parameter indicating the slope of the critical state line.

$\dot{\varepsilon}^{acc}$ is the magnitude of the rate of accumulated permanent strains, that can be computed as [5,6]:

$$\dot{\varepsilon}^{acc} = f_{ampl}\dot{f}_N f_e f_p f_Y f_\pi \tag{17}$$

In Eq. (17), function f_{ampl} indicates the influence of input strain amplitude on permanent strains; f_p considers the influence of the average octahedral pressure, p^{av}; and f_y incorporates the influence of the average stress ratio $\overline{Y}^{av}$ using Matsuoka–Nakai's formulation [32]. The influence of void ratio on permanent strains, f_e, is introduced using a formulation similar to the classical relations for the void ratio dependence of dynamic stiffness proposed by Hardin and Drnevich [33]. f_e has been evaluated with the initial void ratio, not considering, on the side safety, compaction during the cycles; whereas $\dot{f}_N$ indicates the influence of the number of cycles. It is the derivative of function f_N which is formulated as the sum of a linear and a logarithmic term. Variable g^A in the $\dot{f}_N$ expression, see Table 2, accounts for previous cyclic loading, weighting the number of previous cycles with their amplitudes. The expression is $g^A = f^{ampl}\, C_{N1}\, ln(1 + C_{N2}\, N^{eq})$, when, as in our case, the 'equivalent number of equal-strain cycles' N^{eq} is defined (see Section 5.4). The function $f_N = C_{N1}\ [\ln(1 + C_{N2}\ N^{eq}) + C_{N3}\ N^{eq}]$ can only be used if a constant strain amplitude is calculated or if cycles with different amplitudes are grouped into packages. In the latter case, the equivalent number of cycles N^{eq} has to be re-calculated at the beginning of each package – referring to the strain amplitude of the actual package. Finally, f_π considers the influence of a change of cyclic load direction, as it increases the cumulative strains

Table 2
Summary of HCA functions and model parameters [5].

Influence parameter	*Function*	*Material constants*	*Reference values*
Strain amplitude	$f_{ampl} = \min\left\{\left(\frac{\epsilon^{ampl}}{\epsilon^{ampl}_{ref}}\right)^2 ; 100\right\}$		$\epsilon^{ampl}_{ref} = 10^{-4}$
Cyclic preloading	$\dot{f}_N = \dot{f}^A_N + \dot{f}^B_N$ $\dot{f}^A_N = C_{N1} C_{N2} e^{[-g^A/(C_{N1} f_{ampl})]}$ $g^A = f^{ampl} C_{N1} \ln(1 + C_{N2} N^{eq})$ $\dot{f}^B_N = C_{N1} C_{N3}$	C_{N1},C_{N2},C_{N3}	
Void ratio	$f_e = \frac{(C_e - e)^2}{1+e} \frac{1+e_{ref}}{(C_e - e_{ref})^2}$	C_e	$e_{ref} = e_{max}$
Average octahedral normal stress	$f_p = e^{[-C_p(p^{av}/p_{ref} - 1)]}$	C_p	$p_{ref} = p_{atm} = 100$ kPa
Average stress ratio	$f_Y = e^{(C_Y \bar{Y}^{av})}$ $\bar{Y}^{av} = \frac{Y-9}{Y_c - 9}$; $Y_C = \frac{9 - \sin^2\phi_c}{1 - \sin^2\phi_c}$ $Y = -\frac{I_1 I_2}{I_3}$	C_Y	
Polarization changes	$f_\pi = 1 + C_{\pi 1}(1 - \cos\alpha)$ $\dot{\alpha} = -C_{\pi 2}\alpha(\dot{\epsilon}^{ampl})^2$	$C_{\pi 1}$ $C_{\pi 2}$	

[6,34–36]. (In our case, $f_\pi = 1$ since dynamic load always keeps the same kind of vibratory motion over time). Further details of the model are discussed by [5,6].

Table 2 lists 'material constants' for each function in Eq. (17). Therefore, parameters C_e, C_p, C_Y, C_{N1}, C_{N2}, and C_{N3} need to be determined, as well as the critical friction angle (to compute $\boldsymbol{m}$) and the soil´s elastic parameters. Also, to apply the HCA model in real cases, its assumptions and experimental ranges need to be checked for model validity. For instance, f_{ampl} is valid for strain amplitudes below 10^{-3}; for larger amplitudes, the increase of accumulated strains is almost independent of strain amplitude [5,6]. Similarly, experimental results with a wide range of load frequencies up to 20–30 Hz [6,37,38] suggest that the influence of frequency is very small; therefore, although the gas turbine reaches frequencies up to 60 Hz during operation, it will be considered that the influence of vibratory frequency on permanent deformations is still negligible–in other words, it is assumed that the influence of frequency is only through dynamic amplification due to inertial loads. Furthermore, the validity of f_Y functions is confirmed experimentally for p^{av} between 50 and 300 kPa. In our case, the foundation applies an average vertical stress of 66.16 kPa to the subsoil (obtained dividing the weight W, equal to 25,700 kN, by the foundation area of 388.4 m^2). Using Eqs. (18) and (19) – which provide the average vertical stress σ_z and the average horizontal stress σ_x (with $\sigma_y = \nu(\sigma_x + \sigma_z)$ being the average stress for zero lateral strain in the y-direction) integrating Flamant´s Equations [39] for an stress increment due to line loading applied at depth $z=0$ on an elastic halfspace– it is obtained that this is equivalent to an average octahedral normal stress of 51.72 kPa. Therefore, the static stress at any point in the subsoil can be computed adding the geostatic stresses due to the soil´s weight (assuming the at-rest pressure coefficient according to Jaky´s formula) to the static stresses due to foundation weight computed at depth z using Eqs. (18) and (19). A maximum average vertical stress of 273.03 kPa at the maximum depth of influence of $1.5B = 13.5$ m is obtained, with an average octahedral normal stress of 173.73 kPa.

$$\sigma_{z,av}(z) = \frac{2Wz^3}{\pi^2 B_{av} L} \int_{-B_{av}/2}^{B_{av}/2} \frac{dx}{\sqrt{(B_{av}/2)^2 - x^2}} \int_{-B_{av}/2}^{B_{av}/2} \frac{ds}{[(x-s)^2 + z^2]^2} \tag{18}$$

$$\sigma_{x,av}(z) = \frac{2Wz}{\pi^2 B_{av} L} \int_{-B_{av}/2}^{B_{av}/2} \frac{dx}{\sqrt{(B_{av}/2)^2 - x^2}} \int_{-B_{av}/2}^{B_{av}/2} \frac{(x-s)^2 ds}{[(x-s)^2 + z^2]^2} \tag{19}$$

Similarly, f_p was experimentally validated for $\eta^{av} = q^{av}/p^{av}$ between −0.5 and 1.313, and all regions of the field of influence below our foundation present values within such interval. In addition, although the experimental program presented in [5,6] covers dynamic tests with up to 10^5 cycles only, predictions are extended up to 2×10^6 cycles in this case study to consider a more extended period of operation. (Note, however, that 2×10^6 cycles are still only representative of equipment´s operation for a few hours after start-up; although the methodology could be extended beyond that range of cycle numbers, predictive uncertainties would increase, as the HCA model is not validated beyond the number of cycles employed in the experiments. Further details are available at [7].)

5. Implementation and results

5.1. Introduction and model parameters

The existence of analytical solutions for Barkan´s equations depend on the specific types of load-frequency variations with time. For harmonic loads with constant frequency (i.e., corresponding to a stationary regime) an analytical solution exists; however, transient relationships (e.g., as it happens during start-up) require numerical methods. In any case, once the amplitudes of displacement are known, the dynamic stresses and strains that the foundation transmits to the ground can be obtained. Then, based on such stresses and strains, we aim to compute the permanent displacements of the gas turbine foundation. Additional considerations to apply the HCA model in our case are discussed below.

First, we consider the influence of cyclic loads with different directions – remember that there are three modes of vibration, producing vertical and horizontal deformations – and, to apply the HCA model, it will be assumed that the influence of the foundation is equivalent to the vector sum of amplitudes in both directions. Such assumption produces conservative results, as it yields an upper bound of accumulated strains [5].

Similarly, the geometry of the foundation in our case (see Fig. 2) is irregular, so that representative dimensions of its different parts or sections need to be defined. For instance, an average foundation width of 9.07 m is considered; similarly, the distance from the base of the foundation to the rotation axis is taken as 4.24 m.

Next, HCA model parameters need to be estimated. To this end, since the granulometry and index properties of our soil are within the ranges of soils tested for model development, recommendations for model calibration [7] can be followed. For instance, rates of accumulated strains increase with decreasing initial relative density, [24,38] and, for constant initial density, with decreasing particle size d_{50} [7,40]. Furthermore, they increase significantly as the uniformity coefficient increases [7]. Such experimental results lead Wichtmann et al. [7] to conclude that HCA model parameters depend mainly on granulometry (uniformity coefficient, C_u, and effective average size, d_{50}), and index properties (e_{min}). They also proposed a simplified procedure to estimate parameters for the HCA model [7]. (Of course, improved estimates can be obtained when project specific testing results are available). Applying the recommended procedure [7], the following model parameters are obtained for the granular soil under the turbine's foundation: $C_e=0.38$, $C_p=0.59$, $C_Y=2.60$, $C_{N1}=7.42\cdot10^{-3}$, $C_{N2}=2.41\times10^{-2}$ and $C_{N3}=7.17\times10^{-5}$.

5.2. Discretization of strain distributions

To allow a direct implementation into spreadsheet software, the field stress and strain distributions are discretized (into $n_t=20$ layers) over a 'depth of influence' below the foundation given by 1.5 times its width. Thus, assuming a linear distribution of (elastic) strains produced by the vibratory equipment below its foundation (Fig. 6), the total elastic strain amplitude ε_i^{amp} of layer n_i is computed from the strain amplitude at the base of the foundation, ε^{amp}, as:

$$\varepsilon_i^{amp}=\varepsilon^{amp}\left(1+\frac{1-n_i}{n_t}\right) \tag{20}$$

The strain amplitude ε_i^{amp} at the top of each layer is used as a conservative assumption (see Fig. 3). The amplitude at the soil surface, ε^{amp}, entering Eq. (20) is the double of the average result obtained from the dynamic calculation, i.e. from Eq. (13).

From Eq. (20), it is straightforward to compute the total elastic displacement, s_t, as:

$$s_t=\sum_1^{n_t}\varepsilon_i^{amp}L_i \tag{21}$$

where L_i is the thickness of each 'layer' into which the depth of influence is divided. Eq. (21) will also be used to evaluate the accumulated deformation computed with the HCA model, with ε_i^{acc} replacing ε_i^{amp}.

5.3. Solution for the stationary regime

The process can be summarized as follows: The double of the total strain amplitude obtained from the dynamic analysis is treated as the total strain amplitude ε^{amp} at the soil surface. The strain amplitudes of the other layers are then computed from Eq. (20). For each layer, the average stress (p^{av}, Y^{av}) is computed, considering both the soil's own weight and the additional stresses applied by the weight of the machine and of its foundation. For each layer, a separate calculation with the HCA model is performed, i.e. each layer has separate values of f_{ampl}, f_p, f_N, ε^{acc}. See also Table 4, where only one value, corresponding to the top layer, is given for each function.

From these considerations, one can compute permanent deformations accumulated due to stationary operation of the turbine, with a rotation frequency of 60 Hz, which produces an equivalent centrifugal force of 192.54 kN (Eq. (1)). Using parameters $\alpha_x=1.00$; $\alpha_z=2.00$; $\alpha_\theta=0.40$ for Barkan´s model (estimated from [8] using the underlying ground geometry and dynamic properties), the results presented in Table 3 are obtained. Then, using the resulting (input) total strain amplitude ($5.60\cdot10^{-8}$), $\varepsilon^{amp}=2\times5.60\times10^{-8}=1.12\times10^{-7}$ is employed to compute accumulated strains after 2 million cycles, which results in a permanent horizontal deformation of $3.99\cdot10^{-3}$ mm and a permanent vertical deformation (settlement) of 7.02×10^{-3} mm (see Table 4). Therefore, the stationary regime produces strain amplitudes that lead to small permanent deformations (displacements), as it would be expected for a correct foundation design. (Note that "displacements" is used instead of "settlements" because the accumulation direction, given by $\boldsymbol{m}$, is not vertical. Vertical settlements could be obtained projecting it in the vertical direction). Dynamic stresses are used to compute the values of $\boldsymbol{m}$, which vary from one soil layer to another by Eq. (16), and an average value of $\boldsymbol{m}$ is used to compute the results discussed above.

5.4. Solution for the transient situation during start-up

For transient situations, Barkan´s equations are solved numerically. As an example, we study the turbine´s start-up, during which frequencies increase from zero to 60 Hz (see Fig. 4). Since they 'traverse' the natural frequencies of the ground, we need to analyze the influence of the resulting vibration amplifications. The solutions (i.e., surface strain amplitudes corresponding to the three modes of vibration) are shown in Figs. 7–9. Then, their vector sum provides conservative estimates of strain amplitudes in the upper ground layer (see Fig. 10). The solution shows that a maximum (elastic) strain amplitude of 1.76×10^{-5} occurs about 60 s after start-up.

When input strain amplitudes are not constant, the HCA model requires that 'sets' of cycles with the same strain amplitude are treated together. Then, the model estimates the accumulated straindue to such a package; if conditions change during cyclic load (e.g., void ratio changes due to slight compaction with increasing number of cycles; or stress or load amplitude changes), the strain amplitude corresponding to the modified conditions should be recomputed. This happens during start-up, when a variable input load frequency produces non-constant strain amplitudes over time. To divide loads into 'equal-amplitude' packets, 'Miner´s rule' [41], which indicates that the ordering of such packages has little impact on the final accumulated strains, can be applied. (This has been confirmed experimentally by Kaggwa et al. [42] for a low number of cycles, and by Wichtmann et al. [41] for a large number).

Being able to pack groups of cycles together speeds up the calculation, since only a few groups with constant amplitudes need to be considered. The effect of varying cyclic load amplitudes has been researched in geotechnical earthquake engineering [43]: for instance, for liquefaction analyses, a random cyclic loading is usually replaced by an equivalent number of cycles with constant amplitude (usually, with 65% of the cyclic load´s maximum amplitude). Following a similar criterion to select packets of 'equal amplitude' cycles, cycles whose amplitude is above a certain percentage of the group´s maximum amplitude are selected (hereafter, this percentage is called "grouping threshold") and such maximum amplitude is employed as representative of the group of cycles. More specifically, and taking the 65% threshold as an example, the grouping procedure is as follows (see Table 5): first, the $N_1=51$ cycles with strain amplitudes exceeding $0.65\times1.76\times10^{-5}=1.14\times10^{-5}$ are selected, with the amplitude 1.76×10^{-5} being considered as representative for this first group; then, the $N_2=64$ cycles with amplitudes between 1.14×10^{-5} and

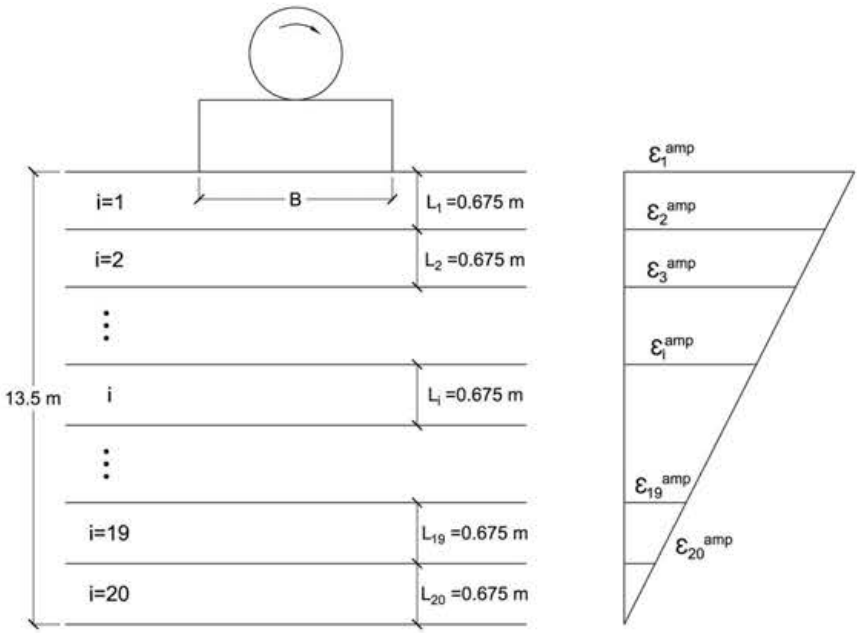

Fig. 6. Example of discretization of the subsoil into 20 layers, showing the and the assumption of linear variation of strain amplitude with depth.

Table 3
Results of Barkan's equations for stationary operation of the machine-foundation dynamic model.

Vertical stiffness constant (kN/m)	$K_z = 15{,}710{,}592$
Horizontal stiffness constant (kN/m)	$K_x = 14{,}296{,}638$
Stiffness constant of rotation (kNm)	$K_\theta = 564{,}868{,}844$
Horizontal displacement amplitude (mm)	5.27×10^{-4}
Vertical displacement amplitude (mm)	$Z = 5.40 \times 10^{-4}$
Amplitude of rotation (rad)	$\theta_y = 1.52 \times 10^{-7}$
Total horizontal displacement amplitude (mm)	$X = 7.97 \times 10^{-4}$
Dynamic horizontal force (kN)	$K_x x = 11.40$
Dynamic vertical force (kN)	$K_z z = 8.48$
Acting moment (kNm)	$K_\theta \theta_y = 86.02$
Horizontal stress due to dynamic horizontal force (kPa)	2.93×10^{-2}
Vertical stress due to dynamic horizontal force (kPa)	3.30×10^{-2}
Vertical stress due to dynamic vertical force (kPa)	2.18×10^{-2}
Horizontal strain amplitude due to dynamic horizontal force	1.89×10^{-8}
Vertical strain amplitude due to dynamic horizontal force (using Eq. (12) and σ_{zh} of Eq. (13))	2.55×10^{-8}
Vertical strain amplitude due to dynamic vertical force (using Eq. (12) and σ_{zv} of Eq. (13))	2.72×10^{-8}
Total strain amplitude	5.60×10^{-8}

Table 4
Example of input parameters and results, for the top layer, of the HCA model for accumulation of permanent strains in stationary regime.

Parameter or variable	***Calculated value***	***Material constants***	***Reference values***
Strain amplitude in the upper layer	$f_{ampl} = 1.25 \times 10^{-6}$		$\epsilon_{ref}^{ampl} = 10^{-4}$
Cyclic preloading in the upper layer	$f_N = 1.14$	$C_{N1} = 7.42 \times 10^{-3}$ $C_{N2} = 2.41 \times 10^{-2}$ $C_{N3} = 7.17 \times 10^{-5}$	
Void ratio	$f_e = 0.25$	$C_e = 0.38$	$e_{ref} = 0.70$
Octahedral average stress in the upper layer	$f_p = 0.58$	$C_p = 0.59$	$p_{ref} = 100$ kPa
Average stress ratio in the upper layer	$f_Y = 2.03$	$C_Y = 2.60$	
Polarization Changes	$f_\pi = 1$		
Cumulative strain in the upper layer	$\epsilon^{acc} = 1.10 \times 10^{-6}$		
Accumulation direction	$\boldsymbol{m} = (0.443,\ 0.443,\ 0.780)$		
Permanent vertical displacement	0.007 mm		
Permanent horizontal displacement	0.004 mm		
Total cumulative displacement	0.009 mm		

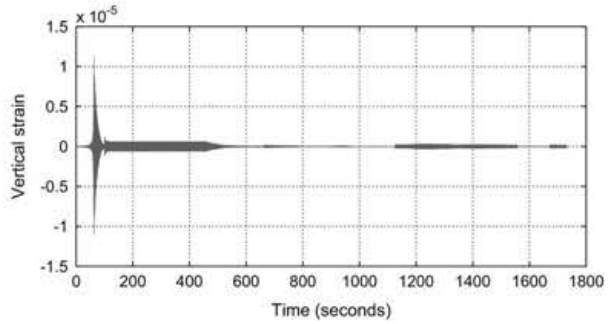

Fig. 7. Surface vertical strains for vertical oscillatory movement during start-up.

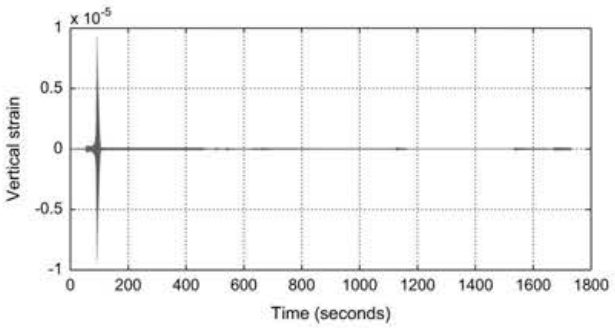

Fig. 8. Surface vertical strains for swinging movement during start-up.

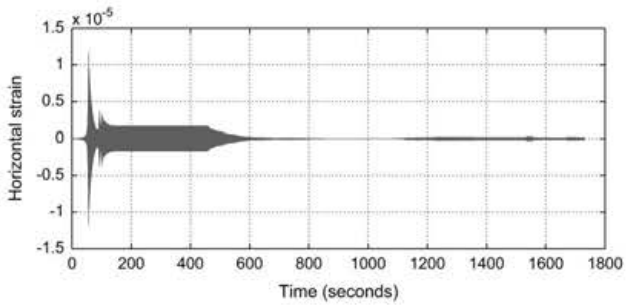

Fig. 9. Surface horizontal strains for swinging movement during start-up.

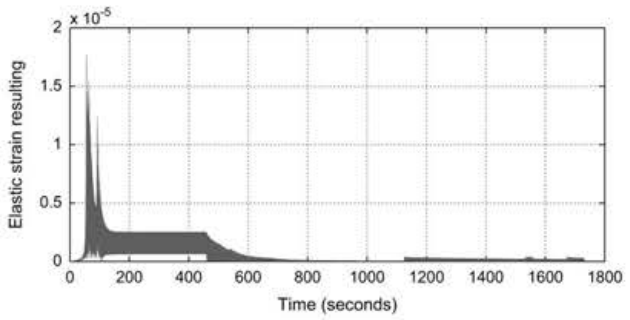

Fig. 10. Total strain amplitude on the ground surface due to dynamic excitations during start-up.

$0.65 \times 1.14 \times 10^{-5} = 7.44 \times 10^{-6}$ are collected, with the representative amplitude of 1.14×10^{-5}, and so on. A value of 65% is initially proposed as grouping threshold; however, since this is heuristic, thresholds of 75% and 90% have also been considered.

Once load cycles have been grouped based on their amplitudes, accumulated strains can be computed using the HCA model. However, since the HCA model prediction depends on the number of cycles, we need to develop the concept of "equivalent number of equal-strain cycles". It represents, for the strain amplitude of the new package, the number of cycles with such amplitude that would have produced the accumulated strain up to that point. Thus, to compute the accumulated strain ε_{i+1}^{acc} produced by a new packet of N_{i+1} cycles with amplitude ε_{i+1}^{amp}, the number of cycles, N_i^{eq}, with amplitude ε_{i+1}^{amp}, to achieve the current accumulated strain ε_i^{acc} is computed first; then, the accumulated permanent strain of interest, ε_{i+1}^{acc}, produced by $N_i^{eq}+N_{i+1}$ cycles of amplitude ε_{i+1}^{amp} is calculated. This treatment of irregular cycles – that implies that subsequent strain accumulation is independent on whether the current permanent strain has been produced by a large number of small amplitude cycles or by a small number of large ones – is consistent with the results of laboratory tests by Gidel et al. [27].

Using the accumulation model with the amplitudes of surface total elastic strains presented in Fig. 10 produces – for grouping thresholds of 65%, 75% and 90% – the results presented in Table 5, where only the first five packages with the greatest strain amplitudes are shown. (The accumulation direction is equal to the stationary case, with $\boldsymbol{m}$=(0.443, 0.443, 0.780)). Therefore, considering packets of cycles defined using the 65% threshold can be considered conservative, since it produces maximum permanent displacements. In this case, a maximum permanent displacement of 0.83 mm is obtained for the start-up situation, therefore exceeding the 0.009 mm computed for the 2 million cycles considered for the turbine´s stationary operation by far. That is, permanent displacements of the turbine foundation are mainly due to the transient situation corresponding to start-up conditions. This observation, that would have gone unnoticed with traditional (heuristic) approaches for dynamic foundation design, emphasizes the importance of considering transient situations for the analysis of foundations with dynamic loads.

6. Conclusions

This paper analyzes permanent displacements of dynamic equipments founded on granular soils. We study a turbine founded on a fine, poorly graded, and medium density sand, for a co-generation plant in the Middle East. Barkan´s equations are solved to compute the (elastic) soil´s response to dynamic loads applied by the turbine, and such results (i.e., the total elastic strain at the ground surface) are employed as input data to estimate accumulated permanent strains produced by the turbine. To that end, a linear variation of (elastic) strain amplitudes with depth is assumed below the foundation; using an appropriate discretization along the foundation´s depth of influence, and the high-cycle accumulation (HCA) empirical model, yields permanent strains produced by (low intensity) cyclic loads that act during the stationary operation of the turbine or during transient situations such as start-up. From such strains, permanent (accumulated) deformations or settlements can be readily computed. The methodology is simple to use, and can be easily implemented using standard mathematical software.

Our example case is solved using typical values for the geometry of the turbine´s foundation based on an available preliminary design. In addition, since granulometry (d_{50} and C_u) and index properties (e_{min}) have the main influence on the HCA´s model parameters for a particular soil, expressions recommended by [7] can be employed, without conducting specific dynamic triaxial tests, to estimate HCA model parameters. For the purpose of selecting equivalent packages that can be used with the HCA model, it has also be shown that a grouping threshold of 65% can be employed to group input (strain) cycles, as it produces adequate (and conservative) results.

Finally, results highlight that, in some cases and for usual design conditions, transient situations (such as start-up) could

Table 5
Results of the HCA model to compute accumulation of permanent strains during start-up, using packages of constant strain amplitude cycles as input for the calculation.

Grouping thresholds corresponding to packets of cycles	*The five greatest intervals of total elastic strain amplitude in the upper layer*	*Number of cycles*	*Permanent strain in the upper layer at the end of all packets of cycles*	*Maximum permanent displacement (mm)*
65%	$(1.14 \times 10^{-5}, 1.76 \times 10^{-5})$ $(7.44 \times 10^{-6}, 1.14 \times 10^{-5})$ $(4.83 \times 10^{-6}, 7.44 \times 10^{-6})$ $(3.14 \times 10^{-6}, 4.83 \times 10^{-6})$ $(2.04 \times 10^{-6}, 3.14 \times 10^{-6})$	51 64 135 340 3475	1.74×10^{-4}	0.83
75%	$(1.32 \times 10^{-5}, 1.76 \times 10^{-5})$ $(1.00 \times 10^{-5}, 1.32 \times 10^{-5})$ $(7.43 \times 10^{-6}, 1.00 \times 10^{-5})$ $(5.57 \times 10^{-6}, 7.43 \times 10^{-6})$ $(4.18 \cdot 10^{-6}, 5.57 \times 10^{-6})$	30 43 34 57 149	1.71×10^{-4}	0.72
90%	$(1.58 \times 10^{-5}, 1.76 \times 10^{-5})$ $(1.43 \times 10^{-5}, 1.58 \times 10^{-5})$ $(1.28 \times 10^{-5}, 1.43 \times 10^{-5})$ $(1.15 \times 10^{-5}, 1.28 \times 10^{-5})$ $(1.04 \times 10^{-5}, 1.15 \times 10^{-5})$	6 16 14 15 11	1.63×10^{-4}	0.70

be more restrictive than stationary situations corresponding to normal operations. This is because of amplification effects: many frequencies are traversed during such transient situations, and they could become (as it happens herein) very similar to the natural frequencies of the ground. (On the side of safety, damping has been neglected.) Therefore, settlement estimations for vibratory equipments with high responsibility should consider accumulated deformations for both their 'steady-state' (or normal) operation and for 'transient-states' such as start-up. In other words, simply checking the validity of the foundation design for the stationary situation (as it often happens in practice) might not be enough to produce a proper foundation design, and accumulated displacements that consider transient situations should be explicitly evaluated.

The analysis presented in this article has excluded damping of the subsoil and the calculated accumulated strains will exceed the actual accumulated strains that would result had damping been considered. Future research in this area should focus on the appropriate inclusion of damping when analyzing system response under transient conditions during start up and shut down.

Acknowledgments

We are indebted to two anonymous reviewers for their comments, which greatly helped us to improve the manuscript. This research was funded, in part, through the collaboration of the IBERDROLA Foundation, through its call for Research on Energy and the Environment Grants Energy for Research.

References

Okur DV, Ansal A. Stiffness degradation of natural fine grained soils during cyclic loading. Soil Dyn Earthq Eng 2007;27:843–54.
Luo W. The characteristics of soils subjected to repeated loads and their applications to engineering practice. Soils Found. 1973;13(1):12–26.
Anyaegbunam AJ. Minimum foundation mass for vibration control. J Geotech Geoenviron Eng 2011;137(2):190–5.
Francois S, Karg C, Haegeman W, Degrande G. A numerical model for foundation settlements due to deformation accumulation in granular soils under repeated small amplitude dynamic loading. Int J Numer Anal Methods Geomech 2010;34:273–96.
Niemunis A, Wichtmann T, Triantafyllidis T. A high-cycle accumulation model for sand. Comput Geotechn 2005;32(4):245–63.
Wichtmann T, Niemunis A, Triantafyllidis T. Strain accumulation in sand due to cyclic loading: drained triaxial tests. Soil Dyn Earthq Eng 2005;25(12):967–79.
Wichtmann T, Niemunis A, Triantafyllidis T. Validation and calibration of a high-cycle accumulation model based on cyclic triaxial tests on eight sands. Soil Found 2009;49(5):711–28.
Barkan DD. Dynamics of bases and foundations. New York: McGraw-Hill; 1962.
Das BM. Principles of soil dynamics. Boston: PWS Kent; 1993.
Iwan WD. On a class of models for the yielding behavior of continuous and composite systems. J Appl Mech 1967;34:612–7.
Mroz Z. On the description of anisotropic workhardening. J Mech Phys Solids 1967;15(3):163–75.
Prevost JH. Undrained shear tests on clays. J Geotech Eng Div 1979;105 (1):49–64.
Valanis KC. A theory of viscoplasticity without a yield. Arch Mech 1971;23:517–35.
Bazant ZP, Krizek RJ. Saturated sand as inelastic two-phase medium. J Eng Mech Div 1975;101(4):317–32.
Cuellar V, Bazant ZP, Krizek RJ, Silver ML. Densification and hysteresis of sand under cyclic shear. J Geotech Eng Div 1977;103(5):399–416.
Dafalias Y.F., Herrmann LR. Bounding surface formulation of soil plasticity. In: Pande GN, Zienkiewicz OC. editors, Soil mechanics transient and cyclic loads; 1982; p. 253–82.
Whittle AJ. Evaluation of a constitutive model for overconsolidated clays. Geotecnique 1993;43(2):289–313.
Pestana JM, Biscontin G, Nadim F, Andersen K. Modeling cyclic behavior of lightly overconsolidated clays in simple shear. Soil Dyn Earthq Eng 2000;19: 501–19.
Kolymbas D, Herle I, Wolffersdorff PA. Hypoplastic constitutive equation with back stress. Int J Numer Anal Methods Geomech 1995;19(6):415–46.
Gudehus G. A comprehensive constitutive equation for granular materials. Soils Found 1996;36(1):1–12.
Bauer E. Calibration of a comprehensive hypoplastic model for granular materials. Soils Found 1996;36(1):13–26.
Pastor M, Zienkiewicz OC. Chan AHC. Generalized plasticity and the modeling of soil behaviour. Int J Numer Anal Methods Geomech 1990;14:151–90.
Anastasopoulos I, Gelagoti F, Kourkoulis R, Gazetas G. Simplified constitutive model for simulation of cyclic response of shallow foundations: validation against laboratory tests. J Geotech Geoenviron Eng 2011;137(12):1154–68.
Marr WA, Christian JT. Permanent displacements due to cyclic wave loading. J Geotech Eng Div 1981;107(GT8):1129–49.
Bouckovalas G, Whitman RV, Marr WA. Permanent displacement of sand with cyclic loading. J Geotech Eng 1984;110(11):1606–23.
Li D, Selig ET. Cumulative plastic deformation for fine-grained subgrade soils. J Geotech Eng 1996;122(12):939–57.
Gidel G, Breysse D, Hornych P, Chauvin J, Denis A. A new approach for investigating the permanent deformation behavior of unbound granular material using the repeated load triaxial apparatus. Bull Lab Ponts Chausséss 2001:233.
Gotschol A, Kempfert HG. Zyklisch viskoelastisch viskoplastischer Stoffansatz nichtbindiger Böden und Schotter. Bautechnik 2004;81(4):279–85.
Sawicki A, Swidzinski W. Mechanics of a sandy subsoil subjected to cyclic loadings. Int J Numer Anal Methods Geomech 1989;14:511–29.
Suiker AJ. The mechanical behaviour of ballasted railways tracks. [PhD thesis]. Holland: Delft University of Technology; 2002.
Wichtmann T. Explicit accumulation model for non-cohesive soils under cyclic loading. [PhD thesis]. Bochum: Publications of the Institute of Soil Mechanics and Foundation Engineering Ruhr-University; 2005.

Matsuoka H, Nakai T. A new failure criterion for soils in three-dimensional stress. In: Proceedings of IUTAM Conference on Deformation and Failure of Granular Materials, Delft;1982 p. 253–63.
Hardin BO, Dmevich VP. Shear modulus and damping in soils: design equation and curves. J Soil Mech Found 1972;98(SM7):667–92.
Yamada Y, Isihara K. Yielding of loose sand in three dimensional stress conditions. Soils Found 1982;22(3):13–31.
Wichtmann T, Niemunis A, Triantafyllidis T. On the infuence of the polarization and the shape of the strain loop on strain accumulation in sand under high-cyclic loading. Soil Dyn Earthq Eng 2007;27(1):14–28.
Wichtmann T, Niemunis A, Triantafyllidis T. Strain accumulation in sand due to cyclic loading: drained cyclic tests with triaxial extension. Soil Dyn Earthq Eng 2007;27(1):42–8.
Thom NH, Brown SF. The effect of moisture on the structural performance of a crushed-limestone road base. Washington: D.C: Transportation Research Board; 1986.
Duku P, Stewart J, Whang D, Yee E. Volumetric strains of clean sands subject to cyclic loads. J Geotech Geoenviron Eng 2008;134(8):1073–85.
Timoshenko SP, Goodier JN. Theory of elasticity. McGraw-Hill, Int. Edn.; 1982.
Castro G, Poulus SJ. Factors affecting liquefaction and cyclic mobility. J Geotechn Eng Div 1977;103(6):501–6.
Wichtmann T, Niemunis A, Triantafyllidis T. Strain accumulation in sand due to drained cyclic loading: on the effect of monotonic and cyclic preloading (Miner's rule). Soil Dyn Earthq Eng 2010;30(8):736–46.
Kaggwa WS, Booker JR, Carter JP. Residual strains in calcareous sand due to irregular cyclic loading. J Geotech Eng 1991;117(2):201–18.
Seed HB, Idriss IM. Simplified procedure for evaluating soil liquefaction potential. J Soil Mech Found Div (ASCE) 1971;97(SM9):1249–73.